

# Stability of periodic domain structures in a two-dimensional dipolar model

Kwok-On Ng and David Vanderbilt

*Department of Physics and Astronomy, Rutgers University, Piscataway, NJ 08855-0849*

(October 4, 2018)

## Abstract

We investigate the energetic ground states of a model two-phase system with  $1/r^3$  dipolar interactions in two dimensions. The model exhibits spontaneous formation of two kinds of periodic domain structure. A striped domain structure is stable near half filling, but as the area fraction is changed, a transition to a hexagonal lattice of almost-circular droplets occurs. The stability of the equilibrium striped domain structure against distortions of the boundary is demonstrated, and the importance of hexagonal distortions of the droplets is quantified. The relevance of the theory for physical surface systems with elastic, electrostatic, or magnetostatic  $1/r^3$  interactions is discussed.

68.35.Rh, 68.35.-p, 68.10.-m, 75.30.Pd

## I. INTRODUCTION

There are a variety of interesting circumstances under which the spontaneous formation of domain structures has been observed or predicted in two-dimensional systems as a result of long-range electrostatic, magnetic, or elastic interactions. For example, several works have shown that electrostatic dipole-dipole interactions are responsible for stabilizing the domain patterns observed in Langmuir monolayers at the water/air interface.<sup>1–5</sup> Similarly, it has been suggested<sup>6,7</sup> that work-function variations could lead to the stabilization of periodic domain structures on metal surfaces such as those observed for partial coverages of oxygen on Cu(110).<sup>8</sup> Closely analogous is the case of thin ferromagnetic films for which the magnetization is normal to the plane of the film.<sup>9–16</sup> Similar effects arise for surface segregation into phases which are not inherently dipolar, but which have different electric or magnetic susceptibilities, in an applied field. For example, dramatic effects have been observed in planar-confined ferrofluid/water mixtures in magnetic fields.<sup>17–20</sup> Finally, it has been understood for some time that surface stress discontinuities at domain boundaries can stabilize domain structures.<sup>21</sup> This effect explains the formation of the herringbone reconstruction of Au(111),<sup>22</sup> provides an alternate explanation of the Cu(110):O domain structures,<sup>6,7</sup> and has far-reaching consequences for Si(100) surfaces.<sup>23,24</sup> A review of some of these effects appears in Ref. 25.

In the above cases, most of the essential physics can be captured in a model with two distinct phases A and B, sharp A–B boundaries having energy per unit length  $\gamma_b$  independent of orientation, and  $1/r^3$  interactions of strength  $K_d$  between a “dipole density”  $\psi_A$  or  $\psi_B$  in domains of type A or B respectively. A model of this form, or a closely related form, has been considered previously by many authors.<sup>4,5,13,15,16,19</sup> For example, for the case of Langmuir films, if  $\psi_A$  and  $\psi_B$  are the screened electric dipole density normal to the water/air interface in the absence and presence of the Langmuir layer, respectively, then  $K_d$  is just  $2\epsilon/(\epsilon + 1)$  (Gaussian units),<sup>4</sup> where  $\epsilon$  is the dielectric constant of the substrate (water). For the case of metal surfaces,  $\epsilon \rightarrow \infty$  so that  $K_d = 2$ , and  $4\pi\psi$  is just the work function.<sup>6</sup> The magnetic

case is analogous to the electric one. For surface stress effects,  $\psi$  is just the surface stress, and  $K_d$  is related to a bulk elastic compliance. (In this case,  $\psi$  and  $K_d/r^3$  have extra tensorial indices and the details become more complicated, but the scaling behavior is the same.<sup>21,23</sup>)

Given the wide range of interesting phenomena which fall within the scope of this model, it is remarkable how little is known theoretically about its behavior. Even the ground-state structure as a function of area fraction  $f = f_A = 1 - f_B$  has not been convincingly established. The case of the simple striped domain structure is well understood,<sup>5,6,13,15,19,21,23</sup> but the stability of this domain structure to oscillatory fluctuations of the domain boundaries remains controversial. Marchenko has predicted that such an instability should occur, speculating that it may lead to an ordered droplet phase.<sup>13</sup> However, recent work of Kashuba and Pokrovsky<sup>15</sup> and Abanov *et al.*<sup>16</sup> does not appear consistent with such an instability. (The demonstration of an instability for a single isolated stripe of non-optimal width<sup>18</sup> does not necessarily imply instability of the equilibrium periodic lattice of stripes as considered here.) Numerical calculations of the relative energy of droplet and striped phases led to a predicted phase transition sequence droplet  $\rightarrow$  striped  $\rightarrow$  inverted-droplet as a function of area fraction  $f$ , with transitions at  $f \simeq 0.28$  and  $0.72$ .<sup>6</sup> These phases are illustrated in Fig. 1(d), (a), and (f), respectively. However, the question of the stability of the striped phase to sinuous distortions such as those shown in Fig. 1(b) and (c) was not addressed in this work. Also, the effects of deviations of the droplet shape from perfect circularity, as in Fig. 1(e), were not assessed.

The purpose of this report is to establish firmly the correct equilibrium phase sequence as a function of area fraction within this model. We first develop the formalism to describe the model in Sec. II. Then in Sec. III, we carefully locate the transition from the striped to the hexagonal-droplet-lattice geometry, and study the coexistence of these two domain structures. In Sec. IV we present numerical calculations which demonstrate that the equilibrium striped phase is stable against undulations of the domain walls at all area fractions, and in Sec. V we show that the expected hexagonal distortions of the droplets in the droplet phase are negligible. Thus, we confirm the basic phase sequence suggested previously.<sup>6</sup> We discuss

the limitations and implications of the work in Sec. VI, and summarize our conclusions in Sec. VII.

## II. DIPOLAR MODEL

### A. Formulation

The energy in this model takes the form

$$E = \gamma_b L_b + \frac{K_d}{2} \int d^2 r \int d^2 r' \frac{\psi(\mathbf{r})\psi(\mathbf{r}')}{|\mathbf{r} - \mathbf{r}'|^3} , \quad (1)$$

where  $L_b$  is the boundary length, and the boundary energy  $\gamma_b$  is assumed to be independent of orientation. As noted above,  $K_d$  is the dipolar coupling constant, and  $\psi(\mathbf{r})$  takes constant values  $\psi_A$  or  $\psi_B$  when  $\mathbf{r}$  lies in an A or B domain, respectively. (We work here at fixed area fraction  $f$ ; one can just as easily work at fixed chemical potential  $\mu$  by introducing the grand potential  $\Omega = E - \mu f A$ , where  $A$  is the system area and  $\mu$  reflects the free energy difference per unit area between the two phases.)

If desired, the second term above can be converted into a double line integral over the boundaries,<sup>13,16,19</sup> and the energy relative to that of uniform phases A and B becomes

$$\Delta E = \gamma_b L_b - \frac{\gamma_d}{2} \int \int \frac{d\mathbf{l} \cdot d\mathbf{l}'}{|\mathbf{l} - \mathbf{l}'|} . \quad (2)$$

Here  $\gamma_d = K_d(\psi_A - \psi_B)^2$ , which has units of energy per unit length like  $\gamma_b$ . When multiple boundaries are present, a double sum over boundaries is understood, and the sense of the line integrals is to be kept uniform (e.g., domain A on the right).

For periodic domain structures, it is convenient to convert to reciprocal space, in which case Eq. (1) or Eq. (2) becomes<sup>6</sup>

$$\Delta F = \gamma_b n_b - \gamma_d \sum_{\mathbf{G}} \pi G |\Theta(\mathbf{G})|^2 . \quad (3)$$

We use  $F$ , as opposed to  $E$ , to represent an energy *density* (energy per unit area), and  $n_b$  is the domain boundary density (length per unit area). The  $\mathbf{G}$  are the reciprocal lattice vectors

of the periodic domain structure under consideration, and  $\Theta(\mathbf{G})$  is the Fourier transform of the function which takes values 0 or 1 inside domains A or B, respectively (or vice versa). Both  $\gamma_b$  and  $\gamma_d$  are assumed to be positive, so that the first term in Eq. (2) or Eq. (3) suppresses domain formation, while the second promotes it.

In each of Eqs. (1-3), logarithmic divergences occur at small length scales. These may be removed by introducing a microscopic cutoff  $a$ , which may have the interpretation of an atomic lattice spacing, a domain wall width, or a film thickness, depending on the physical context. It can be shown to be equivalent to introduce  $a$  into Eq. (1) (for sufficiently small  $a$ ) in the form of a Lorentzian broadening  $(x^2 + a^2)^{-1}$  of the domain walls, or into Eq. (2) in the form of a cutoff that omits  $|1 - I'| < a$  from the integrals, or into Eq. (3) in the form of a damping factor  $\exp(-2Ga)$ .

If an appropriate value of  $a$  is not known *a priori*, it may be assigned an arbitrary value, as long as  $\gamma_b$  is then fixed with respect to a known structure such as a single isolated stripe or disk. From Eq. (2), the energy of a single stripe of width  $w$  is, per unit length,

$$\begin{aligned}\Delta E'_{\text{stripe}} &= 2\gamma_b - 2\gamma_d \lim_{Y \rightarrow \infty} \left[ \int_a^Y \frac{dy}{y} - \int_0^Y \frac{dy}{\sqrt{y^2 + w^2}} \right] \\ &= 2\gamma_b - 2\gamma_d \ln \left( \frac{w}{2a} \right) ,\end{aligned}\tag{4}$$

and the energy of a single circular droplet of radius  $R$  is

$$\begin{aligned}\Delta E_{\text{disk}} &= 2\pi R\gamma_b - \pi R\gamma_d \int_{a/R}^{\pi} \frac{\cos \theta d\theta}{\sin(\theta/2)} \\ &= 2\pi R \left[ \gamma_b - \gamma_d \ln \left( \frac{4R}{ae^2} \right) \right] .\end{aligned}\tag{5}$$

The boundary energy  $\gamma_b$  should be regarded as being defined experimentally through Eq. (4) or (5) after  $a$  has been chosen. There is no real arbitrariness in practice, since  $a$  and  $\gamma_b$  enter all subsequent formulas only in the particular combination  $\gamma_b + \gamma_d \ln(a)$ .

For later reference, it is useful to note that if the energy per unit minority-phase area is minimized for the isolated stripe or disk, one obtains equilibrium sizes  $w_0 = 2l_0/\pi$  and  $R_0 = e^2 l_0/4\pi$ , where we have introduced a new length scale

$$l_0 = \pi a \exp\left(\frac{\gamma_b}{\gamma_d} + 1\right) . \quad (6)$$

(As we will see in the next subsection,  $l_0$  has the interpretation of the stripe width in the equilibrium stripe phase at half filling.) The equilibrium energies per unit minority-phase area are

$$\Delta\tilde{F}_{\text{stripe}} = -\pi \frac{\gamma_d}{l_0} \quad (7)$$

and

$$\Delta\tilde{F}_{\text{disk}} = -\frac{8\pi}{e^2} \frac{\gamma_d}{l_0} . \quad (8)$$

The latter is  $\sim 8\%$  lower in energy. Thus, circular droplets are the favored structure in the dilute limit.

## B. Periodic domain structures

We have found Eq. (3) to be most convenient for calculating the energy per unit area of periodic domain structures. In Ref. 6 it was shown that any given domain structure can be characterized by a dimensionless and scale-invariant constant  $I$  such that

$$\Delta E = \gamma_b n_b + \gamma_d n_b [I + \ln(\pi n_b a)] . \quad (9)$$

$I$  depends only on the geometry, and not the scale, of the domain structure, and can be written

$$I = \lim_{a \rightarrow 0} \left[ -\frac{\pi}{n_b} \sum_{\mathbf{G}} G |\Theta(\mathbf{G})|^2 e^{-2Ga} - \ln(\pi n_b a) \right] . \quad (10)$$

The representation

$$I = \lim_{a \rightarrow 0} \left[ -\frac{\pi}{n_b} \sum_{\mathbf{G}} G |\Theta(\mathbf{G})|^2 e^{-4G^2 a^2} - \ln(\pi n_b a) + \gamma/2 \right] \quad (11)$$

is entirely equivalent, but has improved convergence properties ( $\gamma$  is Euler's constant).<sup>6</sup> Minimizing Eq. (9) with respect to  $n_b$ , and making use of Eq. (6), one finds that the equilibrium value of  $n_b$  is given by

$$n_b^{-1} = l_0 \exp(I) \quad , \quad (12)$$

at which the energy density is

$$\Delta F = -\frac{\gamma_d}{l_0} \exp(-I) \quad . \quad (13)$$

Thus, regardless of domain geometry, the uniform phase is *always* unstable to the formation of a domain structure, although the length scale  $n_b^{-1}$  of this domain structure depends exponentially on the parameters of the model through Eqs. (6) and (13). Note that  $\gamma_d/l_0$  in Eq. (13) sets the energy scale, while  $l_0\Delta F/\gamma_d = -\exp(-I)$  plays the role of a dimensionless energy function.

It is clear from Eqs. (12) and (13) that the domain structure which minimizes  $I$  will have the lowest energy, and will thus be the physical equilibrium structure at zero temperature. For a simple striped phase characterized by area fraction  $f$ , as illustrated in Fig. 1(a), one finds  $I(f) = -\ln \sin(\pi f)$ .<sup>6,21</sup> This has an absolute minimum  $I = 0$  at  $f = 1/2$  for stripes of equal width; for this case  $n_b^{-1}$  is just  $l_0$ , showing that  $l_0$  is just the equilibrium stripe width.

The principle problem to be addressed next is whether other periodic domain structures, such as wavy stripes or droplets, might have lower  $I$  than the simple striped structure, at least in some range of  $f$ .

### III. COMPETITION BETWEEN STRIPE AND DROPLET PATTERNS

In Ref. 6, it was shown that a hexagonal lattice of circles of one phase on a background of the other phase, shown in Fig. 1(d), becomes energetically favorable relative to the striped structure in the vicinity of  $f < 0.28$ . (Of course, by symmetry, the inverted droplet phase of Fig. 1(f) is then favored for  $f > 0.72$ .) We have repeated the calculation of  $I(f)$  for the

droplet lattice, this time using the analytic representation of the 2D Fourier transform of a disk

$$\Theta(q) = \frac{2\pi R}{q} J_1(qR) \quad (14)$$

( $J_1$  is a Bessel function). The results are shown in Fig. 2, where the scale-optimized energies of Eq. (13) of striped and droplet structures are plotted in dimensionless form vs. area fraction  $f$ . It can be seen that the energies of the droplet and striped domain patterns are very close over most of the range  $0 < f < 1/2$ , the deviation at  $f = 1/2$  being no more than  $\sim 5\%$ . The crossover between the two curves is found to occur at  $f_c = 0.286$ . The slopes of the curves at  $f \rightarrow 0$  correspond to the critical values of chemical potential  $\mu$  at which the minority phase disappears. These are given by  $-\pi = -3.142$  and  $-8\pi/e^2 = -3.401$  as per Eqs. (7) and (8) for striped and droplet domains, respectively, and differ by only  $\sim 8\%$ .

Very near the critical area fraction  $f_c$ , the system can lower its energy by phase separating into superdomains of striped and droplet phases having  $f$  slightly greater and less than  $f_c$ , respectively. The coexistence region is determined by the usual common tangent construction applied to the energy function plotted in Fig. 2. The result of this construction is shown in the inset, where an irrelevant linear function has been added to aid visibility. We find that the coexistence region is delineated by a droplet phase at  $f_{c1} = 0.273$  in equilibrium with a striped phase at  $f_{c2} = 0.299$  at  $\mu_c = -1.855$ .

In the region of phase separation,  $f_{c1} < f < f_{c2}$ , the superdomains themselves should in principle order into a periodic domain superstructure, by virtue of the fact that they have slightly different dipole densities  $\psi_{\text{eff}} = \psi_A + f(\psi_B - \psi_A)$ . The theory of Sec. II A applies, now with  $\gamma_d = K_d(\psi_B - \psi_A)^2 \Delta f^2$ , where  $\Delta f = f_{c2} - f_{c1} = 0.026$ , and  $\gamma_b$  is interpreted as the energy per unit length of a superdomain boundary. Thus a striped superstructure is to be expected near the middle of the phase separation region, and droplet superstructures might occur near  $f_{c1}$  or  $f_{c2}$ .<sup>26</sup> (If so, it is even conceivable that these super-phases could phase separate near coexistence into periodic super-super-structures, etc.) However, the energy scale for the superordering would be extremely weak ( $\Delta f^2 < 10^{-3}$ ), and it seems doubtful



whether these superdomain effects could be observed experimentally.

#### IV. STABILITY OF STRIPED PHASES

We now wish to consider the stability of the striped domain phase to perturbations of the boundaries. We will consider both in-phase and out-of-phase fluctuations of the boundary, as sketched in Figs. 1(c) and 1(d), respectively. We let the stripes be propagating along the  $x$ -direction, with unit periodic repeat distance in the  $y$ -direction, and a boundary deviation of the form of

$$y = A \sin(kx) \quad . \quad (15)$$

The problem is to compute  $I(f, k, A)$ , where  $f$  is the area fraction, and  $A$  is the amplitude and  $k$  the wavevector of variation. By symmetry,  $I(f, k, A)$  can be expanded in even powers of  $A$ :

$$I(f, k, A) = I_0(f) + \alpha(f, k)A^2 + \mathcal{O}(A^4) \quad . \quad (16)$$

This equation defines the stiffness  $\alpha(f, k)$  of the domain wall with respect to sinuous displacements. If a negative value of  $\alpha$  were found, it would indicate instability of the striped domain structure.

We first develop a method for calculating  $\alpha(f, k)$  directly. The perturbed structure is periodic with lattice vectors  $2\pi\hat{x}/k$  and  $\hat{y}$ , and reciprocal lattice vectors  $\mathbf{G} = km\hat{x} + 2\pi n\hat{y}$ , so that the Fourier components appearing in Eq. (3) can be written  $\Theta(\mathbf{G}) = \Theta(m, n)$ . Expanding in powers of  $A$  and keeping only terms up to order  $A^2$ , we find for the case of in-phase variation of the domain boundaries

$$\Theta(0, n) = \frac{e^{-in\pi}}{n\pi} (1 - \pi^2 n^2 A^2) \sin(\pi n f) \quad (17)$$

and

$$\Theta(\pm 1, n) = \mp e^{-in\pi} A \sin(\pi n f) \quad , \quad (18)$$

with all other Fourier components vanishing. Equation (10) then leads to

$$\alpha(f, k) = \sum_{n=1}^{\infty} \sin^2(\pi n f) \left[ e^{-4n\pi a} \left( \frac{k^2}{2n} + 4\pi^2 n - 2\pi a k^2 \right) - 2\pi \sqrt{(2\pi n)^2 + k^2} e^{-2\sqrt{(2\pi n)^2 + k^2} a} \right] . \quad (19)$$

Introducing  $\kappa = k/2\pi$  and taking the limit  $a \rightarrow 0$ ,

$$\alpha(f, \kappa) = \sum_{n=1}^{\infty} 4\pi^2 \sin^2(\pi n f) \left[ \frac{\kappa^2}{2n} + n - \sqrt{n^2 + \kappa^2} \right] , \quad (20)$$

which can be proved by careful expansion of the exponential factors in Eq. (19). The three terms appearing in the bracket above result from the increase of  $n_b$ , the decrease of the  $\Theta(0, n)$  components, and the increase of the  $\Theta(\pm 1, n)$  components, respectively, with  $A$ . Since the first two terms are always larger in magnitude than the third term, we can see that  $\alpha$  is always positive. The results for  $\alpha(\kappa)$  are plotted for  $f = 1/2$  in Fig. 3. In the limit  $\kappa \rightarrow 0$ ,  $\alpha$  is directly proportional to  $\kappa^4$ , while for very large  $\kappa$ ,  $\alpha$  scales as  $\kappa^2 \ln(\kappa)$ . These limiting behaviors are illustrated in Fig. 4. In particular, we find that  $\alpha \simeq 1.052\pi^2 \kappa^4$  for  $\kappa \rightarrow 0$ , and  $\alpha \simeq \pi^2 \kappa^2 \ln(\kappa)$  for  $\kappa$  large, at  $f = 1/2$ .

We use  $\alpha'(f, k)$  to denote the corresponding stiffness for the case of out-of-phase variation, Fig. 1(c). For this case, the  $m = 0$  elements of  $\Theta$  are still given by Eq. (17), while (18) becomes

$$\Theta(\pm 1, n) = i e^{-in\pi} A \cos(\pi n f) . \quad (21)$$

We now find, as  $a \rightarrow 0$ ,

$$\alpha'(f, \kappa) = \sum_{n=1}^{\infty} 4\pi^2 \left[ \sin^2(\pi n f) \left( \frac{\kappa^2}{2n} + n \right) - \cos^2(\pi n f) \sqrt{n^2 + \kappa^2} \right] . \quad (22)$$

The series is conditionally convergent and has to be summed carefully. The results for  $f = 1/2$  are shown as the dashed line in Fig. 3. It can be seen that  $\alpha' > \alpha$  (and thus  $\alpha' > 0$ ) over the entire range of wavevector; this was also found to be the case at other area fractions  $f$ . For  $f = 1/2$  the minimum occurs at about  $k = 4\pi/3$ .

Very recent work of Abanov *et al.*<sup>16</sup> contains a similar stability analysis which appears to confirm these results for the special case of half filling. Our Eqs. (20) and (22) with  $f = 1/2$  correspond to their Eq. (A23) with  $p_x = 0$  and  $\pi/L$ , respectively.

We have further checked the above results numerically by carrying out a direct numerical evaluation of Eq. (11). For this we do not want to rely on an analytical Fourier transform of  $\Theta(\mathbf{r})$ , so we begin by specifying  $\Theta(\mathbf{r})$  directly on a real-space mesh covering the unit cell of interest. To avoid artifacts of the discreteness of the lattice, the function  $\Theta'(\mathbf{r})$  that we actually evaluate on the mesh is a Gaussian-smeared version of  $\Theta(\mathbf{r})$ ,

$$\tilde{\Theta}(\mathbf{r}) = \frac{1}{2} \left[ 1 + \operatorname{erf} \left( \frac{d}{2\sqrt{2}a} \right) \right] , \quad (23)$$

where  $\operatorname{erf}(x)$  is the error function and  $|d|$  is the distance from the domain boundary to  $\mathbf{r}$ , the sign of  $d$  depending on whether  $\mathbf{r}$  is in domain A or B. Since this corresponds to convoluting with a Gaussian function in real space, we have in reciprocal space

$$\tilde{\Theta}(\mathbf{G}) = \Theta(\mathbf{G}) e^{-2G^2 a^2} . \quad (24)$$

In practice,  $\tilde{\Theta}(\mathbf{G})$  is computed by fast Fourier transform. Then the sum in Eq. (11) can be computed simply as  $\sum_{\mathbf{G}} G |\tilde{\Theta}(\mathbf{G})|^2$ . We found that good numerical accuracy was obtained using  $\sim 1024$ – $2048$  grid points in the  $y$ -direction, and an equal mesh density in the  $x$ -direction. The calculated values of  $I(A)$  were then fitted to a quartic polynomial in  $A$  in order to determine  $\alpha$  or  $\alpha'$ . The values determined by this approach match very well with those computed from Eqs. (20) and (22), as shown in (Fig. 3) for  $f = 1/2$ . The errors are typically  $\sim 3\%$  or less. Moreover, by using this approach, we confirm that the surface energy change per unit area increases monotonically with  $A$  in all cases considered. This provides additional evidence, above and beyond the linear-response  $\mathcal{O}(A^2)$  analysis, that the equilibrium in-phase and out-of-phase striped domain structures are always stable with respect to domain boundary variations.

## V. HEXAGONAL DISTORTION OF DROPLETS

We now consider in more detail the domain phase consisting of a hexagonal lattice of droplets. There is no reason to expect the droplets in this phase to be exactly circular; the interactions with neighboring droplets should give rise to some amount of hexagonal distortion, not considered in the previous section, as shown in Fig. 1(e). Are these distortions important? For example, do they lower the energy of the droplet phase significantly with respect to the striped phase, perhaps even eliminating the striped phase from the phase diagram altogether? On the contrary, we show here that the effects of the distortion are insignificant.

We thus consider boundary distortions of the form

$$r = r_0 + A \cos(6\theta) \quad , \quad (25)$$

where  $r$  and  $\theta$  are polar coordinated measured from the center of the droplet,  $r_0$  is its unperturbed radius, and  $A$  is the amplitude of variation. Unlike the case of the striped phase, there is no symmetry which requires  $I(f, A)$  to be an even function of  $A$ , so we expect its Taylor expansion in  $A$  will contain linear as well as higher-order terms. Because there is no simple analytic method to calculate  $\Theta(\mathbf{G})$  for given  $f$  and  $A$ , we again specify  $\Theta(\mathbf{r})$  first on a real space mesh, fast Fourier transform to reciprocal space, and evaluate Eq. (11) in  $G$ -space. We find that a  $2048 \times 2048$  mesh in the parallelogram unit cell gives sufficient numerical accuracy to calculate  $I(f, A)$ . Linear and quadratic coefficients in  $A$  are obtained from a simple fit to a series of calculations using different values of  $A$ , and used to locate the equilibrium distortion  $A_{\min}$  and the corresponding energy change  $\Delta I = I_{\min} - I_0$  at  $A_{\min}$ .

We have carried out such calculations at many values of  $f$ , but it is sufficient to report the results at  $f = 1/2$  (where the striped phase has maximum stability) and at  $f = 0.28$  (near the crossover between the droplet and striped phase). For the cases of  $f = 0.5$  and  $f = 0.28$ , we find  $A_{\min}/r_0 = \sim -3 \times 10^{-3}$  and  $\sim -2 \times 10^{-3}$ , and  $\Delta I = -1.3 \times 10^{-4}$  and  $-2.6 \times 10^{-4}$ ,

respectively. We find  $A_{\min} < 0$  for all  $f$ , which with our conventions indicates that the boundaries try to avoid each other. This causes the portions of the droplet boundary which directly face other droplets to become flattened, as indicated (in exaggerated fashion) in Fig. 1(e). In principle, higher harmonics such as  $\cos(12\theta)$  should be considered in Eq. (25), but given the smallness of the fundamental  $6\theta$  distortion, these are virtually certain to be negligible as well.

The effect of this  $\Delta I$  on the relative stability of the striped and droplet domain phases is miniscule. We estimate that the critical filling fraction  $f_c$  which separates the droplet and striped phases is shifted by only  $\sim 10^{-4}$  due to the distortion of the droplets. Thus, the exact values of  $f_c$ ,  $f_{c1}$  and  $f_{c2}$  of Sec. III are only very slightly shifted, and the description of the transition is virtually unchanged.

## VI. DISCUSSION

While the model that we have studied is motivated by the experimental work summarized in the Introduction, it should be emphasized that extensions of various kinds would probably be needed to make real contact with experiment in most cases.

Perhaps the closest experimental realization of the model can be found in the case of Langmuir layers at the air-water interface. Experimental work on this system has shown indications of the presence of both droplet and striped phases, although it is not clear that the transition between them is connected experimentally with a change in area fraction.<sup>1-3</sup>

Probably the most serious limitation of the model is the assumption that the boundary energy  $\gamma_b$  is independent of orientation. While this is clearly correct for the case of Langmuir layers at the air-water interface, and for ferrofluid mixtures. But it is clearly not correct at crystal surfaces. For example, the striped domains observed on the Cu(110):O surfaces always run along the  $[001]$  direction,<sup>8</sup> presumably because  $[110]$  boundaries are much lower in energy than  $[1\bar{1}0]$  ones. Anisotropy in  $\gamma_b$  will always favor striped domains over droplet or inverted-droplet domains, so the effect of a weak anisotropy will be to shift the critical

area fractions for droplets closer to  $f = 0$  and  $f = 1$ . A strong anisotropy will eliminate the droplet and inverted-droplet phases from the phase diagram altogether.

Another limitation is that in some of the physical situations discussed, the idealization of a pure two-dimensional model is not quite appropriate. For example, for the work on confined ferrofluids and epitaxial ferromagnetic films, the film thickness plays a definite role, giving rise to specific forms of the effective interaction between A and B domains and eliminating the need to introduce an *ad hoc* real-space cutoff  $a$ . In the case of Coulomb interactions in an electrolytic background,<sup>27</sup> screening can convert the  $r^{-3}$  interaction into a short-ranged form, while for the elastic case, the surface stress  $\psi$  and the elastic interaction  $K_d/r^3$  carry extra tensorial indices.<sup>21,23</sup>

Also, we have assumed that the dipole density  $\psi$  always takes on two discrete values  $\psi_A$  and  $\psi_B$ . In some cases we may prefer to think in terms of a model in which there is an intrinsic energy density  $F(\psi)$  having local minima at  $\psi = \psi_A$  and  $\psi_B$ , but for which variations of  $\psi$  from these minima are allowed. For the case of Langmuir layers at the air-water interface, for example, the molecular density in the Langmuir layer is sure to be somewhat compressible.

Moreover, in some cases our characterization of the domain boundary as infinitely sharp may be inappropriate. For example, in the case where phases A and B arise from phase segregation, the boundary is expected to become broad near the phase-separation critical temperature. In such cases also, it is appropriate to treat  $\psi(\mathbf{r})$  as a continuous field, using a Landau-type expansion to describe the energy of the system and the appearance of domain structures.<sup>4</sup>

For atomic-scale magnetic systems, it might be appropriate to go over to a description in terms of lattice spin models, instead of insisting on a continuous  $\mathbf{r}$ -space. The simplest such model would be an Ising model on a square 2D lattice with ferromagnetic nearest-neighbor and antiferromagnetic  $r^{-3}$  long-range exchange interactions. (Unless a specially-tuned second-neighbor interaction is introduced into such a model, the anisotropy of the boundary energy is again likely to favor striped phases aligned along the Cartesian

directions.) We are not aware of previous studies of such a model.

Even assuming the formulation of the model is correct for the system of interest, it would be very desirable to generalize the above zero-temperature theory to finite temperature. The energy scale for defects in the domain structures (e.g., vacancies or interstitials in the droplet phase, stripe terminations in the striped phase) is  $\gamma_d l_0$ , so it is natural to introduce a dimensionless temperature  $t = k_B T / \gamma_d l_0$ . Thus, the problem reduces to mapping out the phase diagram in the  $f - t$  (area-fraction-temperature) plane. This remains an ambitious program for future work. However, we can make the following speculations. We certainly expect a solid-to-liquid melting transition in the droplet phases, quite possibly via the Kosterlitz-Thouless mechanism, with a narrow hexatic phase interposed. The melting temperatures should vanish at  $f \rightarrow 0$  or  $1$ , since the interactions between droplets becomes very weak in those limits. Theoretical considerations suggest that the striped domain structure will melt at any non-zero temperature, giving rise to a 2D nematic phase characterized by an orientational correlation length and having exponential and algebraic decay of positional and orientational order, respectively.<sup>3,15,29</sup> (Further discussion for the case of anisotropic  $\gamma_b$  appears in Refs. 15,16.) The nature of the low-temperature part of the phase diagram near  $f_c$  is especially unclear.

Finally, even assuming that the model is correct and that we know its equilibrium behavior, there may be many circumstances under which the kinetic behavior is more important than the thermodynamics. In fact, we may expect sizable energy barriers to the coalescence or pinching off of droplets, or the formation and annihilation of stripe crosslinks. Some studies of the dynamics of phase separation<sup>27,28</sup> and fingering<sup>19,20</sup> in dipolar systems have already appeared. Nevertheless, even in cases where kinetic effects dominate, it may be of interest to understand the equilibrium phase diagram first, in order to understand the driving forces for the dynamic effects observed.

## VII. SUMMARY AND CONCLUSIONS

In summary, we have carried out a theoretical study of the stability of periodic striped and droplet domain structures for a simple two-dimensional dipolar model at zero temperature. It is confirmed that the striped structure is stable near area fraction  $f = 0.5$ , with transitions to droplet and inverted-droplet structures at  $f = 0.286$  and  $f = 0.714$ , respectively. A small phase-separation region near the striped-to-droplet transition was identified. The stability of the striped structure against sinuous displacements of the domain boundaries was confirmed, and the hexagonal distortion of the droplets in the droplet phase was quantified and found to be negligible.

The characterization of the finite-temperature phase diagram of the model, and its kinetic evolution, remain as challenging problems for future study. Furthermore, application to some experimental systems may require refinements of the model, such as an orientation-dependence of the domain-wall energy, a finite film thickness, a finite domain-wall thickness, a compressibility of the dipole density, or addition of tensorial indices for the elastic case. Nevertheless, it is hoped that the present work will provide a firm foundation for future developments.



## REFERENCES

- <sup>1</sup> M. Seul and M.J. Sammon, Phys. Rev. Lett. **64**, 1903 (1990).
- <sup>2</sup> M. Seul, Physica A **168**, 198 (1990).
- <sup>3</sup> M. Seul and V.S. Chen, Phys. Rev. Lett. **70**, 1658 (1993).
- <sup>4</sup> D. Andelman, F. Brochard and J.-F. Joanny, J. Chem. Phys. **86**, 3673 (1987).
- <sup>5</sup> D.J. Keller, H.M. McConnell and V.T. Moy, J. Phys. Chem. **90**, 2311 (1986).
- <sup>6</sup> D. Vanderbilt, Surf. Sci. Lett. **268**, L300 (1992).
- <sup>7</sup> V.I. Marchenko, JETP Lett. **55**, 73 (1992).
- <sup>8</sup> K. Kern, H. Niehus, A. Schatz, P. Zeppenfeld, J. George and G. Comsa, Phys. Rev. Lett. **67**, 855 (1988).
- <sup>9</sup> R. Allenspach, M. Stampanoni, and A. Bischof, Phys. Rev. Lett. **65**, 3344 (1990); and R. Allenspach and A. Bischof, *ibid.* **69**, 3385 (1992).
- <sup>10</sup> C. Kooy and U. Enz, Phillips Res. Rep. **15**, 7 (1960).
- <sup>11</sup> M. Seul and R. Wolfe, Phys. Rev. A **46**, 7519 (1992); *ibid.*, 7534 (1992).
- <sup>12</sup> T. Garel and S. Doniach, Phys. Rev. B **26**, 325. (1982)
- <sup>13</sup> V.I. Marchenko, Sov. Phys. JETP **63**, 1315 (1986).
- <sup>14</sup> Y. Yafet and E.M. Gyorgy, Phys. Rev. B **38**, 9145 (1988).
- <sup>15</sup> A.B. Kashuba and V.L. Pokrovsky, Phys. Rev. Lett. **70**, 3155 (1993); and Phys. Rev. B **48**, 10335 (1993).
- <sup>16</sup> Ar. Abanov, V. Kalatsky, V.L. Pokrovsky, W.M. Saslow, Phys. Rev. B **51**, 1023 (1995).
- <sup>17</sup> R.E. Rosensweig, *Ferrohydrodynamics* (Cambridge University Press, Cambridge, 1985), and references therein.

- <sup>18</sup> A.O. Tsebers and M.M. Maiorov, *Magnetohydrodynamics* **16**, 21 (1980).
- <sup>19</sup> S.A. Langer, R.E. Goldstein, and D.P. Jackson, *Phys. Rev. A* **46**, 4894 (1992).
- <sup>20</sup> A.J. Dickstein *et al.*, *Science* **261**, 1012 (1993).
- <sup>21</sup> V.I. Marchenko, *JETP Lett.* **33**, 381 (1981); *JETP* **54**, 605 (1981).
- <sup>22</sup> S. Narasimhan and D. Vanderbilt, *Phys. Rev. Lett.* **69**, 1564 (1992).
- <sup>23</sup> O.L. Alerhand, D. Vanderbilt, R.D. Meade and J.D. Joannopoulos, *Phys. Rev. Lett.* **61**, 1973 (1988); **62**, 166 (1989).
- <sup>24</sup> D. Vanderbilt, O.L. Alerhand, R.D. Meade and J.D. Joannopoulos, *J. Vac. Sci. Technol. B* **7**, 1013 (1989).
- <sup>25</sup> D. Vanderbilt, in *Computations for the Nano-Scale*, P. E. Blöchl, A.J. Fisher, and C. Joachim, eds. (Kluwer Academic, 1993), p. 1.
- <sup>26</sup> For the superdomain theory, the boundary energy  $\gamma_b$  becomes orientation-dependent. This will tend to favor striped superdomain structures, and it is thus not clear whether droplet superdomain structures will appear in the phase diagram.
- <sup>27</sup> L.Q. Chen and A.G. Khachaturyan, *Phys. Rev. Lett.* **70**, 1477 (1993).
- <sup>28</sup> M. Seul, *J. Phys. Chem.* **97**, 2941 (1993).
- <sup>29</sup> J. Toner and D.R. Nelson, *Phys. Rev. B* **23**, 316 (1981); D.R. Nelson and J. Toner, *ibid.* **24**, 363 (1981).

## FIGURES

FIG. 1. Striped domain phase: (a) unperturbed, (b) with in-phase, and (c) with out-of-phase boundary displacement, Eq. (15). Droplet phase: (d) unperturbed; (e) with hexagonal boundary displacement, Eq. (25). (f) Inverted droplet phase.

FIG. 2. Comparison of dimensionless energy per unit area, optimized with respect to scale, for striped (solid line), droplet (long dashed), and inverted droplet (short dashed line) domain structures, as a function of area fraction  $f$ . Inset illustrates common tangent construction which determines the phase coexistence region.

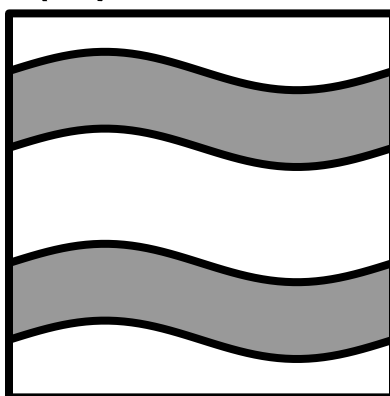
FIG. 3. Stiffness  $\alpha$  vs. reduced wavevector  $\kappa$  for striped phase at filling  $f = 1/2$ . Solid and dashed lines denote in-phase and out-of-phase boundary variations, as computed from Eqs. (20) and (22), respectively. Triangles and circles indicate the corresponding results obtained numerically by finite differences from calculated values of  $I(f, k, A)$  using the method of Eqs. (23)-(24).

FIG. 4. Stiffness vs. wavevector for in-phase boundary variations, from Eq. (20), illustrating asymptotic form for large and small  $\kappa$ . Results are expressed as  $\alpha/\kappa^2$  vs.  $\kappa^2$  for three values of area fraction  $f$ .

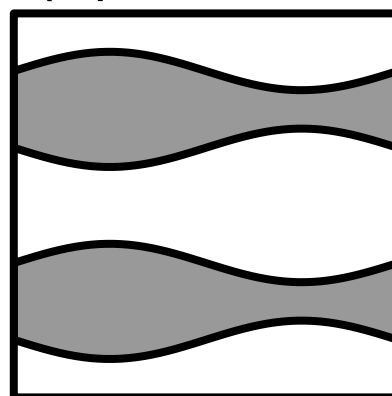
(a)



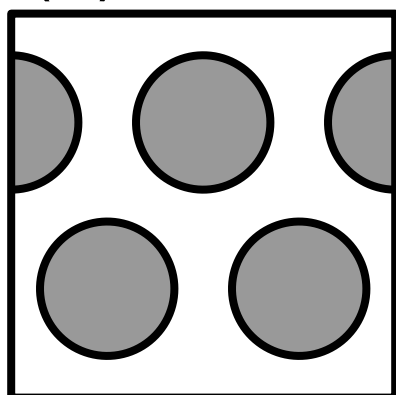
(b)



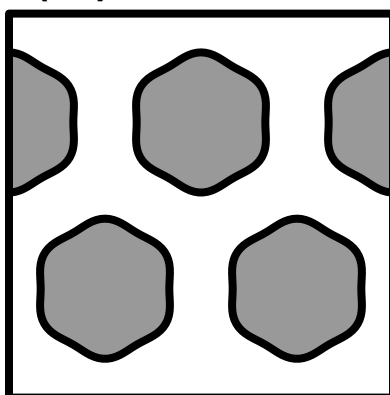
(c)



(d)



(e)



(f)

